

Solid State EXAFS and Luminescence Studies of Neutral, Dinuclear Gold(I) Complexes. Gold(I)–Gold(I) Interactions in the Solid State

William B. Jones,^{1a,b} Jie Yuan,^{1a} Ratnavathany Narayanaswamy,^{1c} Michelle A. Young,^{1c}
R. C. Elder*,^{1a} Alice E. Bruce*,^{1c} and Mitchell R. M. Bruce*,^{1c}

Departments of Chemistry, University of Cincinnati, Cincinnati, Ohio 45221, and University of Maine, Orono, Maine 04469

Received March 16, 1994[⊗]

A series of neutral, dinuclear gold(I) complexes, containing phosphine and thiolate ligands, have been studied by EXAFS and luminescence spectroscopy. Gold(I)–gold(I) interactions are detected for the first time by EXAFS studies on solid samples at liquid helium temperature. A strong, distinct peak at $1.90 \pm 0.02 \text{ \AA}$, assigned to Au–P and Au–S bonds, appears in the Fourier transform for complexes 1–8. A less intense peak appears for complexes 2–6 at 2.8 \AA with the amplitude maximizing toward high k characteristic of a gold backscattering atom. The calculated EXAFS results indicate gold(I)–gold(I) distances ranging from 3.0 to 3.2 \AA for complexes 2–6. In contrast, no gold(I)–gold(I) interactions are detected for complexes 1, 7, and 8. The Au–Au and Au–P(S) distances calculated by EXAFS are similar to those measured by X-ray diffraction. All of the neutral, dinuclear gold(I) complexes luminesce at room temperature in the solid state. The Stokes shifts average $6 \times 10^3 \text{ cm}^{-1}$ and are indicative of a large distortion in the excited state compared to the ground state. Spectral acquisition using time delays of 10–50 μs confirms the phosphorescent nature of the emission. The origin of the luminescence of complexes 1–8 is consistent with a $S \rightarrow \text{Au}$ CT excited state that is perturbed by substituent electronic effects leading to the red shift in emission for 5–8 relative to 1–4. There is no correlation between gold(I)–gold(I) bonding and the energy or band shape of the excitation and emission of 1–8. The luminescence and EXAFS results taken together demonstrate that a gold(I)–gold(I) interaction is not a necessary condition for luminescence. Further, the presence of a gold(I)–gold(I) interaction does not significantly perturb the luminescence in this series of gold(I) complexes. $[\text{Au}_2(p\text{-tc})_2\text{L}]$: $p\text{-tc} = p\text{-thiocresol}$; L = 1,2-bis(diphenylphosphino)ethane (1), 1,3-bis(diphenylphosphino)propane (2), 1,4-bis(diphenylphosphino)butane (3), 1,5-bis(diphenylphosphino)pentane (4). $[\text{Au}(\text{L})(\text{pdt})\text{Au}]$: $\text{pdt} = 1,3\text{-propanedithiol}$; L = 1,2-bis(diphenylphosphino)ethane (5), 1,3-bis(diphenylphosphino)propane (6), 1,4-bis(diphenylphosphino)butane (7), 1,5-bis(diphenylphosphino)pentane (8).

Introduction

An interesting phenomenon in gold chemistry that intrigues both theoretical and experimental chemists, is the propensity for closed shell, d^{10} gold(I) atoms to form weak bonding interactions.² These interactions are typically identified by means of X-ray diffraction experiments in which the internuclear distance between gold atoms is less than the sum of the van der Waals radii.³ The electronic structure and photophysics of d^{10} metal complexes also continues to be of wide interest.⁴ There are several examples of dinuclear d^{10} gold complexes for which the lowest energy electronic absorption and emission bands are assigned as originating from a metal–metal interaction.⁵ Until recently monomeric gold(I) complexes had been reported to luminesce only in the solid state, not in solution.⁴ These observations resulted in the suggestion that gold(I)–gold(I) interactions can be identified on the basis of characteristic electronic absorption and emission features.

Our work is directed at understanding the electronic structure and reactivity of gold(I) complexes, especially with regard to

the use of gold in antiarthritis drugs.⁶ We recently reported the results of UV–vis, X-ray, and NMR studies on a series of phosphine gold(I) thiolate complexes.^{6a} The lowest energy electronic transitions for complexes 1–8, illustrated in Figure 1, were assigned as $S \rightarrow \text{Au}$ charge transfer. The crystal

[⊗] Abstract published in *Advance ACS Abstracts*, March 1, 1995.

- (1) (a) University of Cincinnati. (b) Current address: Discovery Group, Mallinckrodt Medical Inc., 675 McDonell Blvd., P.O. Box 5840, St. Louis, MO 63134. (c) University of Maine.
(2) (a) For a recent review see: Schmidbaur, H. *Gold Bull.* **1990**, *23*, 11. (b) Pyykkö, P.; Zhao, Y. *Angew. Chem., Int. Ed. Engl.* **1991**, *30*, 604. (c) Balch, A. L.; Fung, E. Y.; Olmstead, M. M. *J. Am. Chem. Soc.* **1990**, *112*, 5181. (d) Raptis, R. G.; Fackler, J. P., Jr.; Murray, H. H.; Porter, L. C. *Inorg. Chem.* **1989**, *28*, 4057. (e) King, C.; Wang, J.-C.; Khan, M. N. I.; Fackler, J. P., Jr. *Inorg. Chem.* **1989**, *28*, 2145. (f) Jiang, Y.; Alvarez, S.; Hoffmann, R. *Inorg. Chem.* **1985**, *24*, 749.
(3) Bondi, A. J. *Phys. Chem.* **1964**, *68*, 441.

- (4) (a) McCleskey, T. M.; Gray, H. B. *Inorg. Chem.* **1992**, *31*, 1733. (b) King, C.; Khan, M. N. I.; Staples, R. J.; Fackler, J. P., Jr. *Inorg. Chem.* **1992**, *31*, 3236. (c) Knotter, D. M.; Blasse, G.; van Vliet, J. P. M.; van Koten, G. *Inorg. Chem.* **1992**, *31*, 2196. (d) Li, D.; Yip, H. K.; Che, C. M.; Zhou, Z. Y.; Mak, T. C. W.; Liu, S. T. *J. Chem. Soc., Dalton Trans.* **1992**, 2445. (e) Balch, A. L.; Catalano, V. J. *Inorg. Chem.* **1991**, *30*, 1302. (f) Perreault, D.; Drouin, M.; Michel, A.; Harvey, P. D. *Inorg. Chem.* **1991**, *30*, 2. (g) Yam, V. W. W.; Lai, T. F.; Che, C. M. *J. Chem. Soc., Dalton Trans.* **1990**, 3747. (h) Balch, A. L.; Catalano, A. L.; Olmstead, M. M. *Inorg. Chem.* **1990**, *29*, 585. (i) Che, C. M.; Kwong, H. L.; Poon, C. K.; Yam, V. W. W. *J. Chem. Soc., Dalton Trans.* **1990**, 3215. (j) Khan, M. N. I.; King, C.; Heinrich, D. D.; Fackler, J. P.; Porter, L. C. *Inorg. Chem.* **1989**, *28*, 2150. (k) King, C.; Wang, J. C.; Khan, M. N. I.; Fackler, J. P. *Inorg. Chem.* **1989**, *28*, 2145. (l) Che, C. M.; Kwong, H. L.; Yam, V. W. W.; Cho, K. C.; *J. Chem. Soc., Chem. Commun.* **1989**, 885. (m) An example of a three-coordinate gold(I) complex, without Au–Au interactions, that exhibits solid state and solution emission was recently reported: Shieh, S.-J.; Li, D.; Peng, S.-M.; Che, C.-M. *J. Chem. Soc., Dalton Trans.* **1993**, 195.
(5) For example see: (a) Che, C. M.; Wong, W. T.; Lai, T. F.; Kwong, H. L. *J. Chem. Soc., Chem. Commun.* **1989**, 243. (b) Markert, J. T.; Blom, G.; Perregaux, A. D.; Nagasundaram, N.; Corson, M. R.; Ludi, A.; Nagle, J. K.; Patterson, H. H. *Chem. Phys. Lett.* **1985**, *118*, 258.
(6) (a) Narayanaswamy, R.; Young, M. A.; Parkhurst, E.; Ouellette, M.; Kerr, M. E.; Ho, D. M.; Elder, R. C.; Bruce, A. E.; Bruce, M. R. M. *Inorg. Chem.* **1993**, *32*, 2506. (b) Jiang, T.; Wei, G.; Turnmel, C.; Bruce, A. E.; Bruce, M. R. M. *Metal-Based Drugs* **1994**, *1*, 405. (c) Foley, J.; Fort, R. C., Jr.; McDougal, K.; Bruce, M. R. M.; Bruce, A. E. *Metal-Based Drugs* **1994**, *1*, 419.

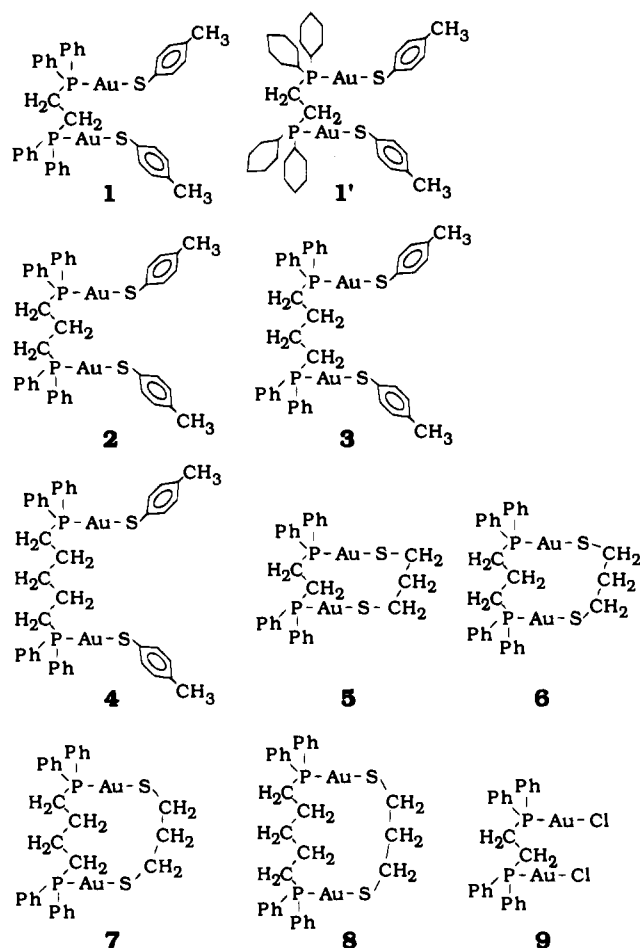


Figure 1. Schematic representation of the series of dinuclear gold(I) complexes 1–9.

structures of **3** and **4** revealed the presence of short intermolecular gold(I)–gold(I) distances of 3.09 and 3.20 Å, respectively. Although analytically pure samples have been prepared for all complexes in Figure 1, X-ray quality crystals have only been obtained for **3** and **4**. In order to obtain more structural information about the remaining complexes, in particular, information about gold–gold interactions, we turned to EXAFS (extended X-ray absorption fine structure). We also investigated the luminescence of **1–8** in the solid state to determine whether gold–gold interactions in these dinuclear complexes correlate with luminescence.

EXAFS is a powerful technique for analyzing the local environment about a specific atom. For example, EXAFS has been successfully used to detect relatively strong interactions at room temperature, such as the Ir–Ir interactions (2.87 Å) in solid $[\text{Ir}(\text{CNMe})_4]\text{Cl}$.⁷ However, weaker interactions, especially those greater than 3 Å, can be difficult or even impossible to detect at room temperature by EXAFS.^{7,8} The origin of this insensitivity lies in thermal disorder which dampens the EXAFS signal amplitude. Decreasing the temperature reduces the disorder and should allow weaker interactions, such as gold(I)–gold(I) interactions, to be detected. We now report EXAFS studies at liquid helium temperature that detect gold(I)–gold(I) interactions in the solid state for the first time. These measurements, together with luminescence studies on dinuclear gold(I) complexes, allow us to examine whether gold(I)–gold(I) interactions perturb the emission spectra.

(7) Carr, N.; Crossley, J. G.; Dent, A. J.; Gouge, J. R.; Neville, G.; Jarrett, P. J.; Orpen, A. G. *J. Chem. Soc., Chem. Commun.*, **1990**, 1370.

(8) Kortright, J. B.; Bienenstock, A. *Phys. Rev. B* **1988**, *37*, 2979.

Experimental Section

Syntheses of 1–9. All manipulations were performed under nitrogen, employing standard Schlenk and glovebox techniques.⁹ Complexes **1–9** were synthesized using previously published methods.^{6a,10}

Abbreviations. The following abbreviations are used: *p*-tc = *p*-thiocresol; pdt = 1,3-propanedithiol; dppe = 1,2-bis(diphenylphosphino)ethane; dppp = 1,3-bis(diphenylphosphino)propane; dppb = 1,4-bis(diphenylphosphino)butane; dpppn = 1,5-bis(diphenylphosphino)pentane; dcpe = 1,2-bis(dicyclohexylphosphino)ethane.

EXAFS. The extended X-ray absorption fine structure (EXAFS) data were collected at the Stanford Synchrotron Radiation Laboratory using the Biostructures beam line IV-3. Transmitted intensity and incident intensity were measured using standard N_2 -filled ionization chambers. Simultaneous calibration of the wavelength was performed by passing the transmitted intensity through a 0.01 mm gold foil standard. The fluorescence data were collected concurrently with the transmission data using a Stern, Heald detector (EXAFS Co.) fitted with a germanium filter to stop scattered radiation. The scans were collected over a range 1000 eV above the Au– L_3 edge to get sufficient data to extract the high *k* information necessary to observe Au–Au bonds. A flowing liquid helium cryostat (Oxford Instruments) was used to cool the samples to approximately 10 K. All EXAFS samples were diluted with boron nitride and placed in a cell with a 1 mm path length. The data were processed using a locally modified version of XFPAC (Robert Scott, University of Georgia).

Luminescence Measurements. Luminescence measurements were made by using a Perkin-Elmer LS-50 luminescence spectrometer. Emission and excitation spectra were not corrected for instrumental response. Solid-state samples were packed into 2 mm quartz capillary tubes and introduced into the Perkin-Elmer variable temperature accessory. All spectra were obtained at room temperature. A 40–50 μs time delay between excitation pulse and emission detection was used to eliminate light scattering and to observe phosphorescence. Slit widths for excitation and emission monochrometers were typically set at 10 nm. Attempts to obtain spectra near liquid nitrogen temperatures were unsuccessful due to instrumental limitations.¹¹

Results and Discussion

XANES. The XANES region of the spectrum can be used as a fingerprint giving useful information about the oxidation state and coordination environment about a central gold atom.¹² Information gained in this region can be used to complement the information extracted from the EXAFS. The features in the XANES region for gold complexes allow us to assign oxidation state and to some extent coordination environment. In the work presented here, each of the spectra for compounds **1–8** show a low, broad peak maximizing at 11 927 eV, which can be unambiguously assigned to a Au(I)–P bond.

EXAFS of Model Compounds. Previous attempts to extract structural information for gold–gold interactions using EXAFS data measured at ambient temperature have failed. We postulate that the reason for failure arises from the thermal disorder in the molecule which severely reduces the EXAFS signal. The

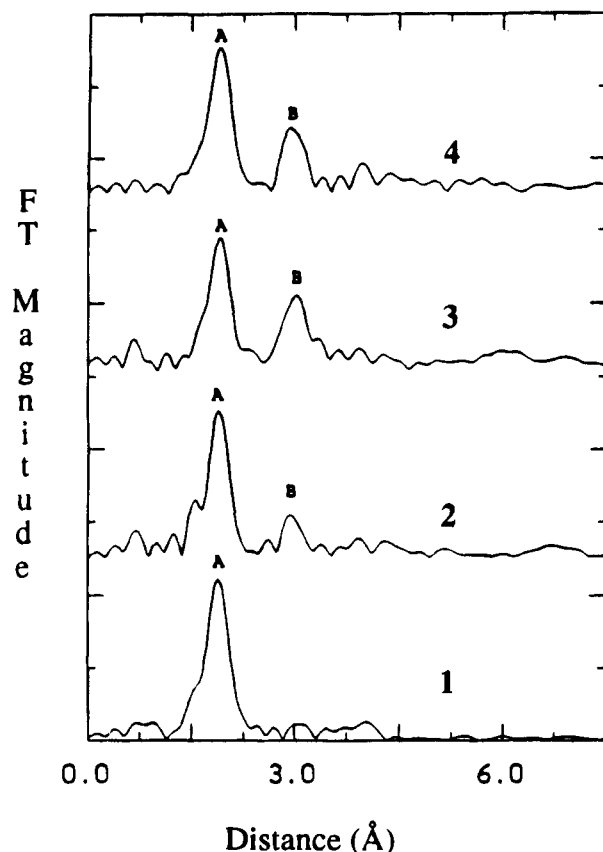
(9) Shriver, D. F.; Drezdon, M. A. *The Manipulation of Air-Sensitive Compounds*, 2nd ed.; Wiley: New York, 1986.

(10) Mirabelli, C. K.; Hill, D. T.; Faucette, L. F.; McCabe, F. L.; Girard, G. R.; Bryan, D. B.; Sutton, B. M.; Bartus, J. O.; Crooke, S. T.; Johnson, R. K. *J. Med. Chem.* **1987**, *30*, 2181.

(11) In our hands, use of the Perkin-Elmer LS-50 instrument at near liquid nitrogen temperatures was limited to very short time periods, due to sample compartment frosting. Several precautions were taken to decrease frosting including: (1) predrying the instrument with dry nitrogen gas for 1–3 h, (2) operation in an air-conditioned room, (3) using 2–5 times the recommended flow rate of dry nitrogen, (4) diverting some of the nitrogen purge gas through an 18 gauge needle aimed directly at the sample tube, and (5) placing the accessory compartment inside a glovebag purged with dry nitrogen. None of these precautions made it possible to obtain reproducible measurements at low temperature.

(12) Elder, R. C.; Eidness, M. K. *Chem. Rev.* **1987**, *87*, 1027.

A.



B.

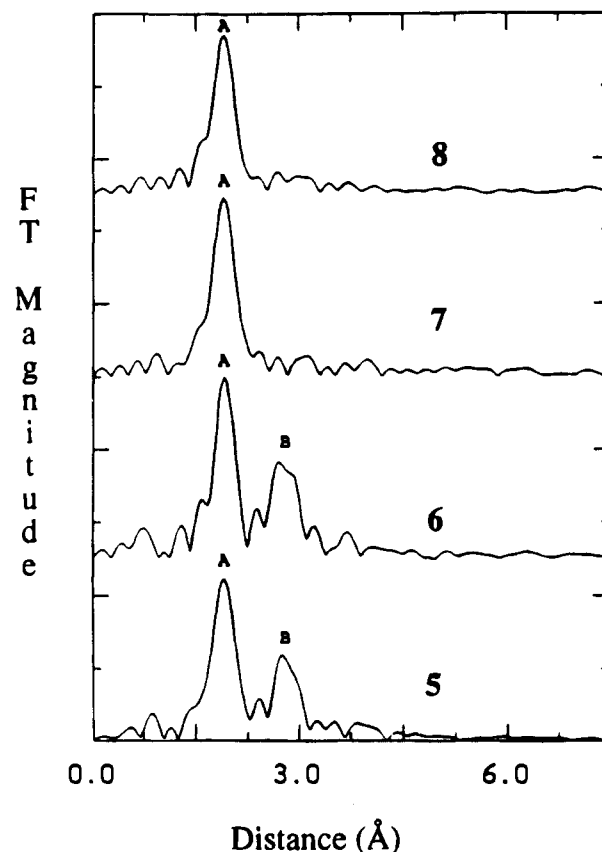


Figure 2. A: Fourier transform magnitude versus distance for complexes 1–4. B: Fourier transform magnitude versus distance for complexes 5–8.

EXAFS signal, $\chi(k)$, is calculated as follows:

$$\chi(k) = \sum_j \frac{N_j}{kr_j^2} (F_j(k)) e^{-2\theta_j^2 k^2} \sin(2kr_j + \phi_j(k)) \quad (1)$$

and

$$k = \left[\frac{2m(E - E_0)}{\hbar^2} \right]^{1/2} \quad (2)$$

where N represents the number of atoms of the j th type at a distance of r contributing to the backscattering; k , the photoelectron wave vector; $F_j(k)$, the calculated amplitude; $\phi(k)$, the calculated phase, and θ , the Debye–Waller factor. The damping in this equation is described by the factor $\exp(-2\theta_j^2 k^2)$. Gold–gold interactions provide their strongest signals at high values of k and therefore are damped to a much greater extent than gold–phosphorus or sulfur bonds. By measurement of the data at reduced temperature (i.e. 10 K) the thermal disorder is substantially decreased and the previously unobserved signal from backscattering atoms becomes observable.

Two compounds for which crystal structures are known were used as model compounds for the EXAFS calculations: $\text{Na}_3\text{[Au(S}_2\text{O}_3)_2]$ ¹³ and $[\text{Au(PCH}_3\text{Ph}_2)_2]\text{PF}_6$.¹⁴ The thiosulfate complex has both Au–S interactions and a longer Au–Au inter-

action. The EXAFS data were modeled with both theoretical parameters derived from Teo and Lee,¹⁵ and empirical parameters were extracted from the models and applied to the data measured for compounds of unknown structure.

The gold–phosphorus and gold–sulfur bonds were easily modeled using EXAFS data measured at ambient temperature for both the model and sample. Structural parameters such as bond distance and coordination numbers were in good agreement with the values determined from single crystal X-ray diffraction using both empirical and theoretical models. Gold–gold interactions ranging between 2.8 and 3.1 Å were not observed in the EXAFS signal measured at ambient temperature, and therefore structural information could not be extracted. Subsequently the data for both model and sample were measured at reduced temperatures. The accuracy of the structural information gained for the gold–phosphorus and –sulfur bonds was not significantly improved. In contrast, the gold–gold interactions, whose signals were not observed in the EXAFS data measured at ambient temperature, could be modeled and structural information gained.

EXAFS of the Dinuclear Gold Compounds. A strong, distinct peak at 1.90 ± 0.02 Å, peak A in Figure 2, appears in the Fourier transform for complexes 1–8. The entire peak was transformed into k space and various models were fit to the data. Gold–phosphorus and gold–sulfur bonds can not be distinguished by EXAFS because of the similarity in P and S electron density and bond distances to gold. Complexes 1–8 were fit as both homoleptic phosphorus and sulfur complexes

(13) Rubin, H.; Zalkin, A.; Faltens, M. O.; Templeton, D. H. *Inorg. Chem.* **1974**, *13*, 1836.

(14) Guy, J. J.; Jones, P. G.; Sheldrick, G. M. *Acta Crystallogr.*, **1976**, *B32*, 1937.

(15) Teo, B.-K.; Lee, P. A. *J. Am. Chem. Soc.* **1979**, *101*, 2815.

Table 1. Sulfur and Phosphorus EXAFS Fit Results for Single Shell Empirical Fits

compound	atom type ^a	r (Å)	CN atoms	θ (Å)	$\Delta E(0)$ (eV)	fit value
Au ₂ (<i>p</i> -tc) ₂ (dppe) (1)	P	2.29 ^b	2.26	0.064	1.0	0.08
	S	2.27	2.14	0.060	-1.1	0.10
Au ₂ (<i>p</i> -tc) ₂ (dppp) (2)	P	2.29	1.76	0.057	0.3	0.08
	S	2.27	1.62	0.054	-1.6	0.16
Au ₂ (<i>p</i> -tc) ₂ (dppb) (3)	P	2.29	1.85	0.060	-0.2	0.14
	S	2.27	1.69	0.057	-1.9	0.08
Au ₂ (<i>p</i> -tc) ₂ (dpppn) (4)	P	2.30	2.21	0.063	1.9	0.09
	S	2.28	2.02	0.060	-0.3	0.08
Au(dppe)(pdt)Au (5)	P	2.29	2.19	0.059	1.9	0.09
	S	2.27	2.00	0.055	-0.1	0.10
Au(dppp)(pdt)Au (6)	P	2.30	1.79	0.049	0.5	0.10
	S	2.28	1.65	0.046	-1.1	0.22
Au(dppb)(pdt)Au (7)	P	2.29	2.26	0.057	1.5	0.17
	S	2.27	2.09	0.054	0.0	0.14
Au(dpppn)(pdt)Au (8)	P	2.29	2.20	0.061	1.5	0.16
	S	2.27	2.02	0.057	-0.5	0.14

^a P = both bound neighbors modeled as phosphorus; S = both modeled as sulfur. ^b Our experience and that of others with single shell EXAFS fits from empirically derived parameters suggests that an esd of 0.01 Å is appropriate for these distances.

using empirical parameters extracted from [Au(PCH₃Ph₂)₂]₂PF₆ and Na₃[Au(S₂O₃)₂]. A comparison of fits is shown in Table 1. The phosphorus model consistently gave bond distances 0.02 Å longer than the sulfur model. The bond distances calculated using phosphorus and sulfur as the empirical models were averaged for the same compound. The average bond distance for complexes 1–3 is 2.28 Å which is the same as the Au–P and Au–S average value calculated from the crystal structure for 3.^{6a} The average bond distance for 4 is 2.29 Å which is also identical to the crystal structure.^{6a} The average bond distance in complexes 5, 7, and 8 is 2.28 Å agreeing with those values for complexes 1–3. The average for all the bond distances is 2.28 ± 0.02 Å which is typical for gold–phosphorus and gold–sulfur bonds. The bond distances do not change significantly as a function of either phosphine ligand backbone length or the type of thiol ligand bound. The coordination number calculation is inherently less accurate than the bond distance calculation. However, all values were within the generally accepted error for two atoms.

A less intense peak, peak B in Figure 2, appears for complexes 2–6 at 2.8 Å. Peak B was Fourier transformed back into *k* space. The amplitude maximizes toward high *k* characteristic of a gold backscattering atom. In contrast there is no peak in this region for complexes 1, 7, and 8. Complex 1 is the shortest open-chain complex studied while complexes 7 and

8 are the largest cyclic complexes studied. These observations suggest that, in the open-chain complexes, the longer bis-(phosphine) chain promotes intermolecular gold–gold interactions possibly as a result of packing energies, entropic effects, or elimination of steric problems. In contrast, the bridging alkanedithiolate creates a cyclic structure that promotes a close gold(I)–gold(I) intramolecular interaction only in the smaller rings.

Both theoretical and empirical parameters were used to model the gold–gold interactions and the results are given in Table 2. Calculations with theoretical parameters consistently give a shorter value for the Au–Au distance than those based on the empirical model by about 0.1 Å.

This probably shows a systematic disparity which results from both models being less than ideal to describe the real case. As can be seen from comparison to the crystal structures, the average of the two types of calculation seems to give a better result than either one taken alone. At the time these calculations were performed the structures of 3 and 4 were unknown. For the two cases subject to test, the average of the calculated EXAFS results agrees with those from the crystal structure within 0.05 Å. The general trend of the distances seems to show that for the cyclic complexes, 5 and 6, the distances are about 3.0 Å, whereas for the open chain, they are above 3.1 Å. More importantly structures 2–6 show a gold–gold interaction, whereas 1, 7, and 8 do not.

Luminescence of Dinuclear Gold(I) Complexes. All of the neutral, dinuclear gold(I) complexes shown in Figure 1 luminesce at room temperature in the solid state. Excitation and emission spectra for the open-chain aromatic thiolate complexes 1 and 2 are shown in parts A and B of Figure 3, respectively. Luminescence spectra for 3 and 4 are very similar in bandshape and energy to those shown (see Table 3). Spectra for the cyclic alkyl dithiolate complexes (shown in Figure 4 for 5 and 8) are also similar to those for the open-chain complexes, with the exception that emission bands are red-shifted for 5–8 (see Table 3). The Stokes shifts average 6 × 10³ cm⁻¹ and are comparable to those for other dinuclear and mononuclear d¹⁰ metal complexes.^{4a–c} A large Stokes shift is indicative of a large distortion in the excited state compared to the ground state and is consistent with phosphorescence. Spectral acquisition using time delays of 10–50 μs confirms the phosphorescent nature of the emission.

The two lowest energy electronic absorptions for complexes 1–8 were previously assigned as S → Au charge transfer.^{6a} Assignment of the emissive excited states in these complexes as predominately LMCT in character is supported by substitution studies. For example, substitution of *p*-thiocresol in 1 (Figure

Table 2. Comparison of EXAFS Results from Empirical, Theoretical, and Crystal Structure Data for Gold(I)–Gold(I) Interactions

compound	results	atom type	dist (Å)	CN atoms	θ^a (Å)	$\Delta E(0)$ (eV)	fit value
Au ₂ (<i>p</i> -tc) ₂ (dppp) (2)	theoretical	Au	3.13	0.64	0.06	23.5	0.13
	empirical ^b	Au	3.22 ^c	0.40	0.05	-16.3	0.12
Au ₂ (<i>p</i> -tc) ₂ (dppb) (3)	theoretical	Au	3.08	0.89	0.05	16.4	0.29
	empirical	Au	3.18	0.71	0.05	-28.9	0.46
	crystal ^{6a}	Au	3.09	1.00			
Au ₂ (<i>p</i> -tc) ₂ (dpppn) (4)	theoretical	Au	3.10	0.79	0.05	25.8	0.11
	empirical	Au	3.20	0.65	0.05	-15.8	0.31
	crystal ^{6a}	Au	3.20	1.00			
Au(dppe)(pdt)Au (5)	theoretical	Au	2.96	0.91	0.05	35.1	0.23
	empirical	Au	3.06	0.72	0.05	-9.1	0.44
Au(dppp)(pdt)Au (6)	theoretical	Au	2.93	1.01	0.05	36.4	0.44
	empirical	Au	3.02	0.77	0.05	-4.9	0.63

^a θ values were held constant throughout the calculations. ^b Empirical utilizes parameters developed from the gold–gold interaction in Na₃[Au(S₂O₃)₂]. ^c Coordination numbers and distances associated with long, weak bonding interactions have large uncertainties associated with them (see Elder, R. C.; Watkins, J. W. *Inorg. Chem.* **1986**, *25*, 223). We estimate the standard deviation in length to be 0.06 Å and the relative standard deviation in the coordination number to be 50% for these cases. The esd's for the two crystal structure distances are less than 0.01 Å.

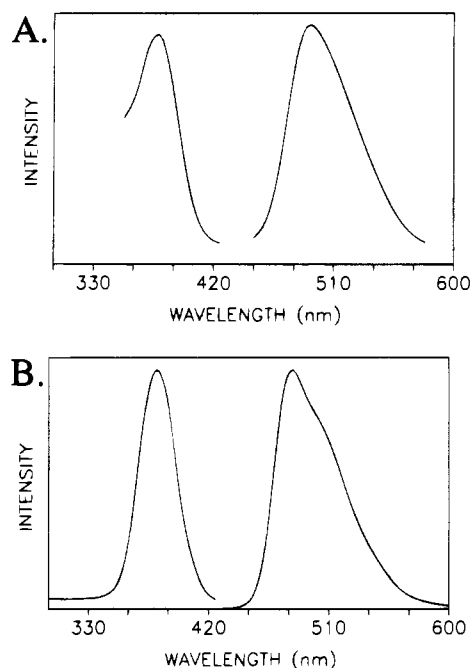


Figure 3. Uncorrected room temperature solid state excitation and emission spectra for (A) $[\text{Au}_2(p\text{-tc})_2(\text{dppe})]$ (**1**) and (B) $[\text{Au}_2(p\text{-tc})_2(\text{dppp})]$ (**2**).

Table 3. Luminescence and EXAFS Data for Au(I) Complexes

complex	luminescence		EXAFS	
	excitation	emission	Au–Au (\AA) ^b	Au–P/S (\AA) ^c
$[\text{Au}_2(p\text{-tc})_2(\text{dppe})]$ (1)	380	495	<i>d</i>	2.28
$[\text{Au}_2(p\text{-tc})_2(\text{dppp})]$ (2)	380	485	3.13	2.28
$[\text{Au}_2(p\text{-tc})_2(\text{dppb})]$ (3)	380	485	3.07	2.28
$[\text{Au}_2(p\text{-tc})_2(\text{dpppn})]$ (4)	375	485	3.10	2.29
$[\text{Au}(\text{dppe})(\text{pdt})\text{Au}]$ (5)	390	515	2.96	2.28
$[\text{Au}(\text{dppp})(\text{pdt})\text{Au}]$ (6)	380	500	2.93	2.29
$[\text{Au}(\text{dppb})(\text{pdt})\text{Au}]$ (7)	395	510	<i>d</i>	2.28
$[\text{Au}(\text{dpppn})(\text{pdt})\text{Au}]$ (8)	390	505	<i>d</i>	2.28
$[\text{Au}_2(p\text{-tc})_2(\text{dcpe})]$ (1')	380	495	<i>e</i>	<i>e</i>
$[\text{Au}_2\text{Cl}_2(\text{dppe})]$ (9)	325	480	<i>e</i>	<i>e</i>

^a Peak maxima were rounded to nearest 5 nm. ^b Average of theoretical and empirical results from Table 2. ^c Average Au–S and Au–P results for single shell empirical fits. ^d No Au–Au interaction was detected. ^e Not measured.

3A) with the more electron donating propanedithiolate ligand in **5** (Figure 4A) results in a red shift in the emission maximum (495 to 515 nm). Similar red shifts in emission energies have formed the basis for assignment of LMCT emissions.¹⁶ The presence of phenyl groups in the bis(phosphine) ligands raises a possible complication since emission bands near 500 nm in phenylphosphine–metal complexes have previously been assigned as originating from $\pi \rightarrow \pi^*$ transitions.¹⁷ However, involvement of phenyl ring orbitals on the bisphosphine or thiolate ligands in emission of **1–8** appears remote for the following reasons: (1) substitution of the dppe ligand in **1** (Figure 3A), with dcpe to form **1'** (Figure 5A), does not significantly alter the luminescence, and (2) replacement of aromatic thiolate ligands with an alkanedithiolate ligand does not significantly alter the luminescence (after taking into account the aforementioned red shift). In addition, substitution of the

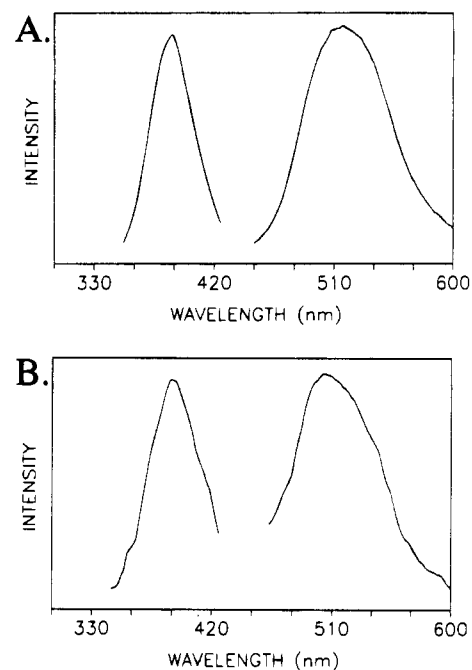


Figure 4. Uncorrected room temperature solid state excitation and emission spectra for (A) $[\text{Au}(\text{dppe})(\text{pdt})\text{Au}]$ (**5**) and (B) $[\text{Au}(\text{dppn})(\text{pdt})\text{Au}]$ (**8**).

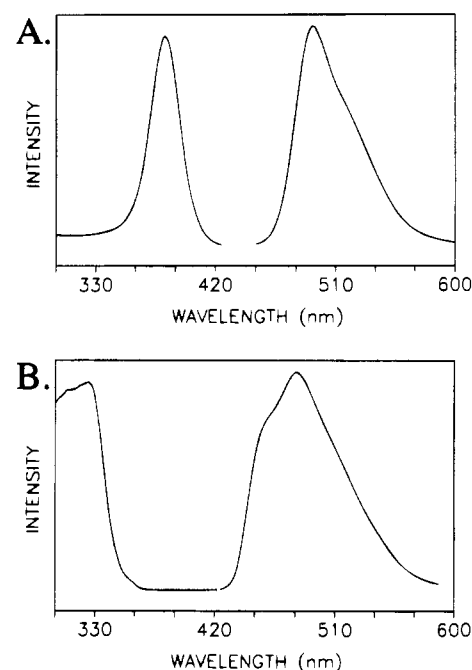


Figure 5. Uncorrected room temperature solid state excitation and emission spectra for (A) $[\text{Au}_2(p\text{-tc})_2(\text{dcpe})]$ (**1'**) and (B) $[\text{Au}_2\text{Cl}_2(\text{dppe})]$ (**9**).

electron rich propane dithiolate ligand in **5** with electron withdrawing chloride atoms to form **9** (Figure 5B), results in a significant blue shift in both the excitation (390 to 325 nm) and emission (515 to 480 nm) maxima.¹⁸ Finally, we note that assignment of S \rightarrow Au charge transfer transitions is consistent with recent assignments of related trinuclear copper(I) arenethiolate complexes as S \rightarrow Cu charge transfer transitions.^{4c}

(16) Paulson, S.; Sullivan, B. P.; Caspar, J. V. *J. Am. Chem. Soc.*, **1992**, *114*, 6905.

(17) Segers, D. P.; DeArmond, M. K.; Grutsch, P. A.; Kutal, C. *Inorg. Chem.* **1984**, *23*, 2874.

(18) Replacement of thiolate with chloride probably results in changing the nature of the electronic transition; i.e., the chloride orbitals are most probably stabilized below filled gold d orbitals.¹⁹ However, the observed blue shift on going from **5** to **9** is still consistent with an LMCT assignment for **5**.

(19) Savas, M. M.; Mason, R. W. *Inorg. Chem.* **1987**, *26*, 301.

EXAFS, Luminescence, and Gold–Gold Interactions. EXAFS spectroscopy is a useful technique for detecting gold–gold interactions in noncrystalline samples where X-ray crystal structure determinations are not feasible. The Au–Au and Au–P(S) distances calculated by EXAFS are similar to those measured by X-ray diffraction. It is interesting to note that complexes **1**, **7**, and **8** do not have gold(I)–gold(I) interactions. Given the pervasive nature of these interactions in the solid state, these three complexes appear to be somewhat atypical.

The origin of the luminescence of complexes **1–8** is consistent with a $S \rightarrow Au$ CT excited state that is perturbed by substituent electronic effects leading to the red shift in emission for **5–8** relative to **1–4** (see Table 3). The luminescence and EXAFS results taken together demonstrate that a gold(I)–gold(I) interaction is not a necessary condition for luminescence. Further, the presence of a gold(I)–gold(I) interaction does not significantly perturb the luminescence in this series of gold(I) complexes. As is shown in Table 3 and Figures 3–5, there is no correlation between gold(I)–gold(I) bonding and the energy or band shape of the excitation and emission of **1–8**. The luminescence spectra of complexes **2–6**, which have gold(I)–gold(I) interactions in the solid state, will not be affected by contributions of the σ and σ^* molecular orbitals (formed by overlap of filled d_{z^2} orbitals on Au) as long as the highest occupied molecular orbital remains sulfur in character.

It is interesting to note that recently, Gray^{4a} and Fackler^{4b} independently reported examples of luminescent *monomeric*

gold(I) complexes that have no gold(I)–gold(I) interactions in solution or in the solid state. Their results show that luminescence in gold(I) monomers can originate from factors not associated with gold(I)–gold(I) interactions. Our results complement those of Fackler and Gray because we have shown that formation of a gold(I)–gold(I) interaction does not necessarily lead to changes in luminescence. The important points are that emission in gold(I) complexes can not be used as a diagnostic test for the presence of gold(I)–gold(I) interactions and that the origin of luminescence in the gold(I) phosphine thiolate complexes reported here is consistent with a $S \rightarrow Au$ CT transition. We are continuing to investigate how the electronic and steric properties of ligands coordinated to gold influence the structure and formation of gold–gold bonds.

Acknowledgment. A.E.B. and M.R.M.B. acknowledge financial support from the National Institutes of Health (Grant AR39858) and the University of Maine BRSG funds. X-ray experiments were carried out at the Stanford Synchrotron Radiation Laboratories which are supported by the Department of Energy using the Biostructures beam line IV-3 which is supported by the National Institutes of Health, Division of Research Resources. W.B.J. thanks the Department of Chemistry at the University of Cincinnati for a Lowenstein-Schubert-Twitchell fellowship.

IC940291A